

ABRA: Teleporting Fine-Tuned Knowledge Across Domains for Open-Vocabulary Object Detection

Mattia Bernardi[✉], Chiara Cappellino[✉], Matteo Mosconi[✉],
Enver Sangineto[✉], Angelo Porrello[✉], and Simone Calderara[✉]

University of Modena and Reggio Emilia
name.surname@unimore.com

Abstract. Although recent Open-Vocabulary Object Detection architectures, such as Grounding DINO, demonstrate strong zero-shot capabilities, their performance degrades significantly under domain shifts. Moreover, many domains of practical interest, such as nighttime or foggy scenes, lack large annotated datasets, preventing direct fine-tuning. In this paper, we introduce **Aligned Basis Relocation for Adaptation (ABRA)**, a method that transfers class-specific detection knowledge from a labeled source domain to a target domain where no training images containing these classes are accessible. ABRA formulates this adaptation as a geometric transport problem in the weight space of a pretrained detector, aligning source and target domain experts to transport class-specific knowledge. Extensive experiments across challenging domain shifts demonstrate that ABRA successfully teleports class-level specialization under multiple adverse conditions. Our code will be made public upon acceptance.

1 Introduction

Recent advances in Open-Vocabulary Object Detection (OVD) demonstrate that Vision-Language Models [25] can localize a broad array of concepts specified at inference time via natural-language prompts, effectively removing the constraint of fixed training categories. Despite this progress, performance often degrades sharply under domain shifts, such as transitions from daylight to low-light scenes or from clear weather to fog. Furthermore, in such adverse scenarios, the acquisition of large, fully annotated detection datasets proves prohibitively expensive or impractical, particularly for rare classes.

Domain Adaptive Object Detection (DAOD) methods typically address this problem by training a detector on a labeled *source* domain and generating pseudo-bounding boxes on unlabeled *target* images for fine-tuning [7, 30]. However, under severe domain shifts (*e.g.*, nighttime imagery), these pseudo labels are often unreliable. Moreover, requiring target-domain images containing all classes of interest – even without bounding-box annotations – implicitly introduces a weak form of supervision, since images must be preselected to ensure full class coverage [28].

In this paper, we propose a distinct adaptation scenario where only a subset of target-domain classes is available during training (*e.g.*, *car*, *bicycle*), while other target classes (*e.g.*, *bus*, *truck*) are labeled exclusively in the source domain, with *no training data available in the target domain*: namely, **neither bounding boxes nor images**. This setting mirrors a common real-world problem in which annotated data are readily available for frequent classes but absent for rare ones. Since standard DAOD approaches are inapplicable to these rare classes, transferring knowledge from a fully labeled source domain becomes essential. Formally, we assume a *source* domain with full supervision across all classes, while the *target*-domain classes are partitioned into *target-available* and *target-unavailable* sets. Our objective is to transfer knowledge from the source domain specifically to the *target-unavailable* classes.

To address the scenario described above, we build upon an OVD backbone (*i.e.*, Grounding DINO [18]) and decompose the adaptation process into two complementary levels of expertise: *domain* and *class*. Within our framework, this decomposition facilitates effective transfer of class-specific knowledge from the *source* to the *target* domain. At the domain level, we introduce *objectification*, a procedure that constructs a class-agnostic *domain expert* designed to capture domain-specific characteristics such as illumination conditions and texture patterns. At the class level, we adapt the technique proposed in [16] to derive lightweight *class experts* that encode category-specific semantic knowledge.

Building on this modular structure, we propose **ABRA (Aligned Basis Relocation for Adaptation)**, a method that transfers class-level knowledge from the source domain to a target domain where no training images of those classes are available. Specifically, ABRA formulates this adaptation problem as a geometric transport in weight space, aligning source and target domain experts through closed-form rotations. The resulting transported class-specific residuals can be plugged into the target-domain expert, thereby forming an effective model without the need to access data for those classes.

We evaluate ABRA on the Cityscapes [5] \rightarrow Foggy Cityscapes [27] transfer; additionally, we examine four further domain shifts within the Single-Source Domain Generalized Object Detection (SDGOD) setting [33], encompassing variations in illumination and weather conditions. Within these benchmarks, we compare our method against several baselines based on transfer learning and weight alignment, demonstrating that ABRA consistently outperforms them across multiple scenarios. In particular, it exhibits strong zero- and few-shot transfer capabilities, providing improved weight initialization for downstream adaptation tasks. In summary, our contributions are as follows:

- We propose a framework that disentangles domain and class knowledge, enabling the relocation of specialized knowledge across domains.
- We introduce ABRA (Aligned Basis Relocation for Adaptation), a mathematically grounded method that transfers class knowledge through domain alignment and class-level residual transport, enabling adaptation to target-domain classes that are absent from the target training set.

- We validate the effectiveness of ABRA across multiple domain shifts, consistently outperforming existing baselines and demonstrating robustness under challenging conditions.

2 Related Work

Open-Vocabulary Object Detection. Open-Vocabulary Object Detection aims to identify and localize object categories beyond those seen during pre-training, allowing users to specify arbitrary classes at inference time via textual prompts. Early approaches [8, 21, 37, 40, 41] align vision and language features using powerful pretrained encoders, such as CLIP [25]. Subsequent works [14, 18] emphasize the use of massive pretraining regimens specifically devised for object detection and incorporate large-scale grounding datasets. Despite their aim to detect nearly any object, these models often exhibit limitations in recognizing rare categories and performing robust detection across diverse domains.

Although previous studies [4, 6] adapt models like Grounding DINO [18] to handle class rarity within Incremental Learning [32], they do not adequately handle the challenge of detecting the same class in different domain contexts. Our paper fills this gap by proposing an adaptation that facilitates across-domain transport by decoupling domain-specific and class-specific semantics.

Modular Deep Learning and Parameter-Efficient Fine-Tuning. Modular Deep Learning [24] contrasts with the traditional monolithic training paradigm by treating neural networks as composable entities that can be adapted selectively. In this spirit, Parameter-Efficient Fine-Tuning techniques (PEFT) have emerged. For instance, LoRA [10] injects low-rank matrices into pretrained backbones, significantly reducing memory requirements for downstream adaptation. LoRA-like methods [13, 15–17, 20, 39] further optimize the trade-off between trainable parameters and performance. SVFT [16], for example, applies low-rank residuals within the SVD subspace of each weight matrix, achieving comparable performance to LoRA with fewer parameters.

We embrace the Modular Deep Learning philosophy, but our approach differs by explicitly separating adaptation into domain-level and class-level modules: a large component handles full domain adaptation, while a smaller, dedicated module encodes class-specific knowledge.

Domain Adaptive Object Detection. Most state-of-the-art DAOD methods rely on the Mean Teacher [31] paradigm, in which a teacher detector generates pseudo-bounding boxes to train a student network [30]. Both networks are initialized from the source detector, with the teacher updated via a moving average of the student’s parameters. Since pseudo-bounding boxes can become unreliable under strong domain shifts, recent approaches employ adaptive data augmentation to mitigate drift toward noisy predictions. For instance, [12] utilizes MixUp [38] to combine bounding boxes from different classes, estimating similarity via a dynamic class confusion matrix. Similarly, [19] blends source and target images using detection uncertainty as mixing coefficients, where uncertainty is modeled by an additional network branch predicting a Gaussian

distribution over box coordinates. In [7], data augmentation is combined with class-specific adaptive thresholds to prune low-confidence boxes and alleviate class imbalance.

Related efforts have explored Single-domain Generalizable Open-Set Object Detection (SG-OSOD) [36], where models must handle domain shifts while grouping completely unseen target objects into a single “unknown” category. In contrast, our approach addresses a fundamentally different challenge: we assume the classes of interest are known and labeled in the source domain but entirely unavailable in the target domain (no images and no labels). Therefore, rather than detecting novelties, we focus on the explicit cross-domain transfer of fine-tuned knowledge to detect these specific categories in adverse target environments (Secs. 1 and 3).

Weight Alignment. Previous literature explores strategies for transporting learned knowledge. Model stitching [2, 9, 23] typically concatenates networks directly, while model rebasin approaches [1, 26, 29] show that fine-tuning modules can be transferred between different pretrained models via weight alignment, such as permutation. In addition, task arithmetic [11, 22] seeks to transport the knowledge of different fine-tuning modules with simple arithmetic operations.

Our strategy is akin to model rebasin: we first compute an optimal rotation that aligns the source and target domain spaces. Then we apply this rotation to the class-specific modules to ensure they are fully compatible with the new target domain. This process enables the direct transport of learned class knowledge from one domain to another.

3 Preliminaries

Problem Setting. Within our framework, we employ a pre-trained Open-Vocabulary detector such as Grounding DINO [18] parameterized by θ_0 . As illustrated in Fig. 1, our objective is to transfer class-specific knowledge from a *source* domain to a *target* domain. In the standard fully supervised setting, each domain is represented

by a dataset of annotated images: $\mathcal{D}_S = \{(x_i^S, y_i^S)\}_{i=1}^{N_S}$ for the source domain and $\mathcal{D}_T = \{(x_i^T, y_i^T)\}_{i=1}^{N_T}$ for the target domain, where x_i denotes an image and y_i its ground-truth object annotations (bounding boxes and class labels).

In our setup, we assume that some categories are unavailable for the target domain. To be formal, we denote by \mathcal{C}_S and \mathcal{C}_T the sets of object classes defined in the source and target domains, respectively. We then partition the target classes into two disjoint sets, *i.e.*, an *available* set $\mathcal{C}_T^{\text{avail}}$ and an *unavailable* set $\mathcal{C}_T^{\text{unav}}$, with $\mathcal{C}_T = \mathcal{C}_T^{\text{avail}} \cup \mathcal{C}_T^{\text{unav}}$ and $\mathcal{C}_T^{\text{avail}} \cap \mathcal{C}_T^{\text{unav}} = \emptyset$. Classes within $\mathcal{C}_T^{\text{avail}}$ are supported by annotated target-domain images, $\mathcal{D}_T^{\text{avail}}$, whereas classes in $\mathcal{C}_T^{\text{unav}} \subseteq \mathcal{C}_S$ are



Fig. 1: Goal. Transfer class-specific knowledge from the source domain to unavailable target classes without access to target-domain data.

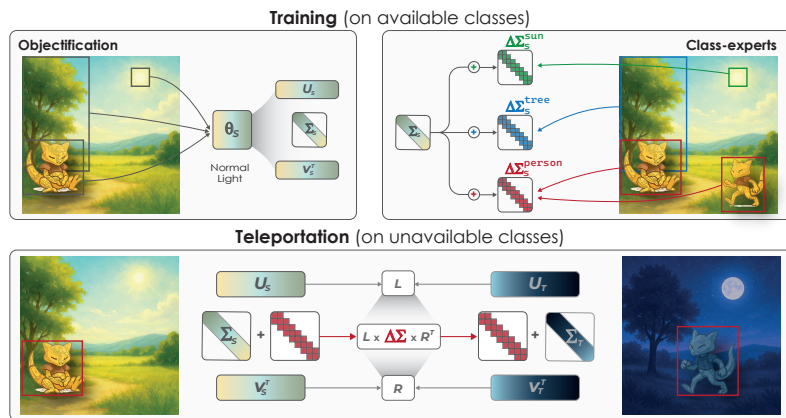


Fig. 2: Overview of the transfer pipeline. Starting from domain experts obtained through Objectification, class-specific residuals learned via SVFT in the source domain are analytically transported to unseen target domains.

observed exclusively in the source domain, lacking any target-domain labels or visual data. This fundamentally differs from the standard DAOD scenario where each class in the target domain has available samples and only lacks supervision.

As exemplified in Fig. 1, where $\mathcal{C}_T^{\text{avail}} = \{\text{tree}, \text{moon}\}$ and $\mathcal{C}_T^{\text{unav}} = \{\text{person}\}$, this configuration mirrors real-world scenarios where rare classes (e.g., a *motorcycle* at night) suffer from a data deficit, while common classes (e.g., a *car* at night) remain readily available. Furthermore, the intersection of $\mathcal{C}_T^{\text{avail}}$ and \mathcal{C}_S is unconstrained and may be either empty or non-empty. We emphasize that the classes targeted for transfer are entirely unavailable in the target domain.

Singular Vectors guided Fine-Tuning. To efficiently specialize our pre-trained detector for novel classes, we leverage Singular Vectors guided Fine-Tuning (SVFT) [16], a parameter-efficient fine-tuning strategy. Rather than updating full weight matrices, SVFT operates within the spectral domain, learning concise residuals $\Delta\Sigma$ on the singular values of a pretrained matrix $\theta_0 = U\Sigma V^T$. This yields the adapted parameterization $\theta_{FT} = U(\Sigma + \Delta\Sigma)V^T$. This compact representation facilitates the creation of lightweight *class modules* that are efficiently transportable across domains.

4 Aligned Basis Relocation for Adaptation

We introduce ABRA, a novel approach designed to transfer class-specific knowledge from a source domain to a target one, achieving this transition entirely without the need for class-specific target-domain data or training iterations. Recent theoretical insights [26] demonstrate that model adaptation can be reformulated as a transportation problem. Embracing this perspective, we begin with the source and target domain modules, θ_S and θ_T , respectively, both of

which are obtained through class-agnostic fine-tuning. We then transport class-specific residuals from the source to the target module. Specifically, we derive a class-specific expert for target class c , denoted as $\theta_S^{(c)} = \theta_S + \tau_S^{(c)}$, where $\tau_S^{(c)}$ represents the residual obtained by fine-tuning solely on class c observed within the source domain. Our ultimate objective is to transfer this fine-tuning displacement, $\tau_S^{(c)} = \theta_S^{(c)} - \theta_S$, onto the target-domain module θ_T , thereby yielding an estimate, $\hat{\theta}_T^{(c)}$, of the ideal detector $\theta_T^{(c)}$. Crucially, this ideal detector corresponds to the model that would naturally result from directly fine-tuning on class c in the target domain, had such data been accessible. Fig. 2 provides a comprehensive illustration of the proposed method.

Organization. In Sec. 4.1, we detail the derivation of the domain expert models, θ_S and θ_T , with the objective of enforcing strong class-agnostic representations. Additionally, Sec. 4.2 outlines the specific procedure employed to derive the class expert, $\theta_S^{(c)} = \theta_S + \tau_S^{(c)}$, within the source domain. Finally, the teleporting process realized by ABRA can be summarized as follows:

$$\hat{\theta}_T^{(c)} = \theta_T + \pi_{S \rightarrow T}(\tau_S^{(c)}), \quad \text{where } \tau_S^{(c)} = \theta_S^{(c)} - \theta_S \quad (1)$$

where $\pi_{S \rightarrow T}(\cdot)$ denotes the transport function that binds the source domain S to the target domain T , as detailed in Sec. 4.3.

4.1 Domain Expert through Objectification

In the upper-left section of Fig. 2, we illustrate the derivation of the domain expert θ_S , which constitutes the first phase of our procedure. We define a domain expert as a detection model that captures the underlying visual statistics of a specific domain (*e.g.*, foggy or rainy weather conditions) while remaining strictly agnostic to individual classes. Our objective is for this model to internalize lighting, texture, and structural characteristics, rather than relying on semantic, class-specific features. To train this domain expert, we introduce a procedure termed *objectification*, depicted in Fig. 3. During this process, the ground-truth annotations of the training set are modified to eliminate class-level supervision, thereby emphasizing domain-level visual cues.

Practically, for each ground-truth bounding box belonging to the *top three most represented* classes, the original semantic label (*e.g.*, **car**, **person**, **bicycle**) is replaced with a single, neutral “**object**” category. This strategy compels the model to locate generic objects of interest rather than identifying their precise classes. Formally, given a specific domain, we construct an objectified dataset \tilde{D}_S by relabeling the bounding boxes of the top three represented classes as “**object**” while discarding all other annotations. Precisely:

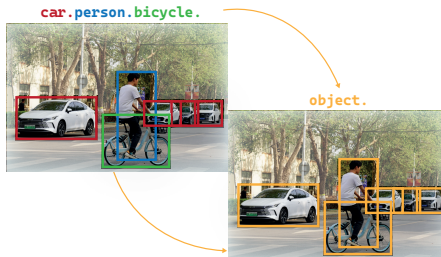


Fig. 3: Objectification. Each domain is fine-tuned using a unified “*object*” label to capture domain appearance.

$$\theta_S = \text{Fine-Tune}(\theta_0, \tilde{\mathcal{D}}_S), \quad \text{where } \tilde{\mathcal{D}}_S = \{(x_i, \text{‘object’})\}_{i=1}^{N_S^{\text{top-3}}} \quad (2)$$

where θ_0 denotes the pretrained parameters of Grounding DINO, x_i represents the input image, and $N_S^{\text{top-3}}$ is the total number of images containing at least one of the three dominant classes. The resulting model, θ_S , serves as the *source domain expert*. An identical procedure is applied to derive the target domain expert, θ_T , and can be generalized to obtain an expert for any domain of interest.

4.2 Class Experts through Singular Vectors

Having established the role and derivation of the domain experts, the subsequent step is to extract class-specific knowledge from the categories intended for transport. For clarity, we continue to refer to the classes originating from the source domain as *source* classes, distinguishing them from the target domain to which they will be transported. However, the following principles apply universally to any class within any domain.

Let $c_S = \text{bus}$ denote a specific class that is supervised in the source dataset but entirely lacks training data in the target domain. Building upon the domain expert θ_S , we aim to train a lightweight, class-specific module specialized in detecting instances of this category. Furthermore, we require this resulting class expert to be fully transportable across domains without necessitating any additional target-domain training.

To achieve this, we first filter the training set by retaining only images that contain at least one instance of the class of interest, and strictly masking out all bounding boxes belonging to any other class. Subsequently, employing the technique detailed in Sec. 3, we efficiently fine-tune a compact residual on top of the domain expert θ_S . Specifically, for a source domain expert weight matrix $\theta_{S,\ell}$ at layer ℓ , we first compute its Singular Value Decomposition, yielding $U_{S,\ell} \Sigma_{S,\ell} V_{S,\ell}^\top$. We then initialize a trainable, class-specific residual matrix $\Delta \Sigma_{S,\ell}^{(c)}$ while freezing the original components $U_{S,\ell}$, $\Sigma_{S,\ell}$, and $V_{S,\ell}^\top$. During optimization, only this minimal residual $\Delta \Sigma_{S,\ell}^{(c)}$ is fine-tuned. The forward pass f for the ℓ -th layer is thus formulated as:

$$f_\ell(x) = \underbrace{U_{S,\ell}}_{\text{frozen}} \left(\underbrace{\Sigma_{S,\ell}}_{\text{frozen}} + \underbrace{\Delta \Sigma_{S,\ell}^{(c)}}_{\text{learnable}} \right) \underbrace{V_{S,\ell}^\top}_{\text{frozen}} x. \quad (3)$$

This training paradigm naturally imposes a low-rank constraint on the residual matrix $\Delta \Sigma_{S,\ell}^{(c)}$. In practice, these residuals can be restricted to a diagonal (parameterized as a vector) or banded (*e.g.*, tri-diagonal) structure. This drastically shrinks the number of learnable parameters required for each class expert, preserving the overall efficiency and compactness of the model.

Upon concluding this fine-tuning phase, we obtain a class-specialized model $\theta_S^{(c)} = \theta_S + \tau_S^{(c)}$ tailored to class c within domain S , as illustrated in the upper-right section of Fig. 2. Moving forward, the isolated residual $\tau_S^{(c)}$ can be utilized

both for direct inference on the source domain and for transportation to an entirely new target domain, as elaborated in the following section.

4.3 Teleportation through Weight Alignment

Equipped with class-agnostic domain experts (θ_S and θ_T) and class-specific residuals $\tau_S^{(c)}$, we now address adaptation to a novel target domain. Our objective is to transfer the knowledge of classes that are entirely unobserved within this new environment. To accomplish this, we introduce a closed-form solution grounded in weight-space rotations, which enables the direct teleportation of class-specific fine-tunings from the source model to the target model. Assuming access to the weight decompositions of both the source class expert and the target class expert, we can define the weights for a given layer ℓ as follows:

$$\theta_{S,\ell}^{(c)} = U_{S,\ell}(\Sigma_{S,\ell} + \Delta\Sigma_{S,\ell}^{(c)})V_{S,\ell}^\top, \quad \theta_{T,\ell}^{(c)} = U_{T,\ell}(\Sigma_{T,\ell} + \Delta\Sigma_{T,\ell}^{(c)})V_{T,\ell}^\top. \quad (4)$$

In this formulation, the target class-specific term $\Delta\Sigma_{T,\ell}^{(c)}$ represents the *unknown*, given that no class-specific data is available from the target domain. However, we do possess the source class expert $\theta_{S,\ell}^{(c)}$ alongside the domain-specific components of the target model — specifically, the singular bases $(U_{T,\ell}, V_{T,\ell})$ derived from the target domain expert θ_T . We leverage these available components to resolve the unknown via a closed-form solution.

Closed-form alignment. For clarity, we omit the layer index ℓ in the subsequent equations. Our core intuition is to rotate the source residual $U_S \Delta\Sigma_S^{(c)} V_S^\top$ into the spectral basin of the target domain (U_T, V_T) , yielding the relation:

$$U_S \Delta\Sigma_S^{(c)} V_S^\top = U_T \pi_{S \rightarrow T}(\Delta\Sigma_S^{(c)}) V_T^\top. \quad (5)$$

To formalize this intuition, we must determine a transformation $\pi_{S \rightarrow T}(\cdot)$ that satisfies Eq. (5). We choose to parameterize such mapping as a bilinear transformation of the source residual:

$$\pi_{S \rightarrow T}(\Delta\Sigma_S^{(c)}) = L \Delta\Sigma_S^{(c)} R^\top, \quad \Rightarrow \quad U_S \Delta\Sigma_S^{(c)} V_S^\top = U_T L \Delta\Sigma_S^{(c)} R^\top V_T^\top, \quad (6)$$

where L and R signify two rotation matrices designed to align the singular subspaces of the source and target domains. The precise values of these matrices can be determined **analytically** by solving the following optimization problems, ensuring the transformation in Eq. (5) remains exact:

$$\min_L \|U_S - U_T L\| \quad \text{s.t. } L^\top L = I, \quad \min_R \|V_S - V_T R\| \quad \text{s.t. } R^\top R = I. \quad (7)$$

Both formulations embody a classic **orthogonal Procrustes problem**, wherein the objective is to discover the optimal rotation matrices L and R that most effectively align the singular vector subspaces across the two domains. The optimal solutions can be straightforwardly obtained in closed form:

$$U_S = U_T L^* \Rightarrow U_T^\top U_S = L^*, \quad V_S = V_T R^* \Rightarrow V_T^\top V_S = R^*. \quad (8)$$

Algorithm 1 ABRA: Aligned Basis Relocation for Adaptation

-
- 1: **Input:** backbone weights θ_0 ; source dataset \mathcal{D}_S ; target dataset \mathcal{D}_T ; class index c .
 - 2: $\theta_S \leftarrow \text{FINE TUNE}(\theta_0, \tilde{\mathcal{D}}_S)$ ▷ Source domain expert via objectification
 - 3: $U_S, \Sigma_S, V_S^\top \leftarrow \text{SVD}(\theta_S)$
 - 4: $\Delta\Sigma_c \leftarrow \text{SVFT}(\theta_S, \mathcal{D}_S^{(c)} = \{(x_i, y_i = c)\})$ ▷ Train class expert on source
 - 5: $\theta_T \leftarrow \text{FINE TUNE}(\theta_0, \tilde{\mathcal{D}}_T)$ ▷ Target domain expert
 - 6: $U_T, \Sigma_T, V_T^\top \leftarrow \text{SVD}(\theta_T)$
 - 7: $(L, R) \leftarrow \text{PROCRUSTES}(U_S, U_T), \text{PROCRUSTES}(V_S, V_T)$
 - 8: $\Delta\Sigma_c^{(t)} \leftarrow L \Delta\Sigma_c R^\top$ ▷ Teleportation through weight alignment
 - 9: $\Sigma'_T \leftarrow \Sigma_T + \Delta\Sigma_c^{(t)}$
 - 10: **return** $\theta_T^{(c)} \leftarrow U_T \Sigma'_T V_T^\top$ ▷ Class-adapted target expert $\theta_T^{(c)}$.
-

Having derived the optimal rotations $L^* = U_T^\top U_S$ and $R^* = V_T^\top V_S$, we can seamlessly teleport the class-specific residual from the source domain directly into the target domain. This procedure yields the definitive formulation for the target-domain class expert:

$$\theta_{T,\ell}^{(c)} \approx U_T(\Sigma_{T,\ell} + \pi_{S \rightarrow T}(\Delta\Sigma_S^{(c)}))V_T^\top \approx U_T(\Sigma_T + U_T^\top U_S \Delta\Sigma_S^{(c)} V_S^\top V_T) V_T^\top \quad (9)$$

A complete derivation and extended discussion of these equations are provided in the supplementary material. In summary, the proposed rotation-based alignment initially constructs a class-specific residual systematically rotated to interface seamlessly with the target expert. Subsequently, we integrate this adapted residual atop the target domain expert. This ultimately yields a highly capable detector equipped to recognize specific classes within the target domain, despite those classes remaining entirely unobserved within the latter. This complete procedure is illustrated in the lower section of Fig. 2 and dissected in Algorithm 1.

5 Experiments

Datasets. As our setting introduces a novel domain transfer paradigm, no standardized benchmark currently exists, to the best of our knowledge. To address this gap, we construct an evaluation framework anchored on two distinct datasets. Our primary benchmark focuses on the widely adopted domain shift from Cityscapes [5] to Foggy Cityscapes [27]. The original Cityscapes dataset provides high-resolution urban street scenes captured under clear weather, while Foggy Cityscapes (0.02 intensity) offers the corresponding scenes rendered with synthetic fog. To further validate our approach across more diverse environmental variations, we employ the SDGOD benchmark [34], which encompasses five distinct weather and lighting conditions: Day-Clear, Day-Foggy, Dusk-Rainy, Night-Rainy, and Night-Clear. It is important to note that we employ only the raw data from these datasets rather than their standard validation protocols. In

our setting, class-level evaluation is performed strictly on the subset of images containing at least one ground-truth instance of the target class, with all other bounding boxes masked out, a fundamental departure from existing benchmarks.

Implementation details. ABRA and the compared baselines all adapt Grounding DINO as the pretrained OVD backbone. Domain checkpoints are derived by fine-tuning only the encoder attention layers for 10 epochs, utilizing a learning rate of $1e-4$ and a batch size of $\mathcal{B} = 2$. Starting from the source-domain expert, we perform class specialization via SVFT by training these same attention layers for an additional 12 epochs with an increased learning rate of $1e-2$ and $\mathcal{B} = 4$. Further details are provided in the supplementary material.

5.1 Benchmarking

To rigorously evaluate our approach, we benchmark against several baselines inspired by recent advancements in task arithmetic. Performance is reported in terms of mAP and AP50; the former represents an average over 10 increasing Intersection over Union (IoU) thresholds, while the latter is computed at a fixed IoU threshold of 50%. These methods are detailed below.

Finetuning (*upper bound*). To establish a theoretical upper bound for our approach, we train a dedicated, fully fine-tuned model for each specific class within the target domain. Starting from θ_0 , we isolate all instances of a given target class c by filtering the target domain dataset to include only images containing class c , and we actively mask out the bounding boxes of any co-occurring non-target classes. By performing standard optimization exclusively on these isolated instances, the resulting specialized model achieves the maximum expected performance for class c , thus serving as our empirical upper bound.

Grounding DINO Zero shot (*baseline*). The frozen pretrained model θ_0 .

Source (*baseline*). This baseline evaluates a model $\theta_{FT}^{(c)}$ directly on the target domain, where $\theta_{FT}^{(c)}$ is obtained by fine-tuning, via SVFT, the pretrained model θ_0 exclusively on class c within the source domain. Since these experts are exposed only to the source distribution of the class c , this setting quantifies the performance degradation caused by transferring a source-trained model to a novel target domain without any adaptation.

Analogy model via Task Arithmetic [11] (*competitor*). As discussed in Sec. 2, Task Arithmetic [11] is a powerful paradigm for constructing new models on the fly, without requiring either examples or additional training steps. For example, it enables building **analogies** between tasks of the form “ A is to B as C is to D .” If the weights of models B , C , and D are known, this paradigm allows us to estimate the weights of model A through simple operations – such as additions and subtractions – performed directly in weight space.

Drawing inspiration from this mechanism, we introduce a straightforward, analogy-based transfer approach to serve as a competitive baseline. Specifically, given the source domain expert θ_S , the target domain expert θ_T , and the source

class expert $\theta_S^{(c)}$, we aim to estimate the weights of the target class expert $\theta_T^{(c)}$ by leveraging the following analogy:

$$\theta_T^{(c)} : \theta_T = \theta_S^{(c)} : \theta_S. \quad (10)$$

In practical terms, as advocated in the original paper, we compute their corresponding task vectors as $\tau_S^{(c)} = \theta_S^{(c)} - \theta_0$, $\tau_S = \theta_S - \theta_0$, and $\tau_T = \theta_T - \theta_0$. The target class model is then obtained by combining these vectors as follows:

$$\theta_T^{(c)} = \theta_0 + \tau_T + \tau_S^{(c)} - \tau_S. \quad (11)$$

Intuitively, starting from the target domain expert, this operation adds the residual information that distinguishes the class expert from the domain expert in the source domain. In other words, we transfer the class-specific deviation learned in the source domain onto the target representation. This arithmetic baseline provides a lightweight reference to assess whether linear composition alone suffices to capture cross-domain class transfer.

Param Δ [3] for Direct Weight Mixing (*competitor*). Recent work in the context of Large Language Models (LLMs) has shown that fine-tuned knowledge can be transferred across different models by directly transporting task vectors. Given a base model θ_A and its fine-tuned counterpart θ_A^* , Param Δ [3] computes the corresponding task vector $\tau_A = \theta_A^* - \theta_A$ and injects it into another model θ_B of the same architecture to obtain $\theta_B^* = \theta_B + \tau_A$. This direct weight-space operation enables transferring task-specific updates across models without requiring any additional training. In our setting, if we treat the two models A and B as the source domain expert θ_S and the target domain expert θ_T , respectively, Param Δ naturally serves as an additional competitor to our approach. In practical terms, this corresponds to using the identity function for the mapping $\pi_{S \rightarrow T}(\cdot)$ from S to T , meaning that no rotation or alignment is applied when transferring the class-specific information. Formally, Param Δ would reduce to:

$$\widehat{\Delta\Sigma}_T^{(c)} = \Delta\Sigma_S^{(c)}, \implies \theta_{T,\ell}^{(c)} \approx U_T(\Sigma_T + \Delta\Sigma_S^{(c)})V_T^\top, \quad (12)$$

which reuses the source residual as-is in the target domain.

5.2 Main Results

Cityscapes \rightarrow Foggy Cityscapes. The results in Tab. 1 highlight the effectiveness of ABRA across all transported classes. All competitors struggle significantly, failing to match the *Source* baseline performance. Specifically, Task Analogy [11] degrades below the Zero shot baseline, while Param Δ [3] offers only marginal gains over zero-shot. In contrast, **ABRA** easily surpasses both baselines and competitors, closely approaching the theoretical upper bound established by full *Fine-tuning*. These results demonstrate that our method effectively transports class-level specialization to the target domain.

Table 1: Cityscapes \rightarrow Foggy Cityscapes. Comparison of mAP and AP₅₀ on unavailable categories. ABRA outperforms all baselines. Best in **bold**.

Method	Bus		Motor		Rider		Train		Truck		Average	
	mAP	AP ₅₀										
<i>Fine-tuning</i>	58.75	73.50	31.22	55.01	43.87	68.06	32.95	58.75	40.03	57.08	41.36	62.48
Zero shot	48.63	61.10	23.20	41.91	18.96	31.70	16.31	44.02	31.20	41.88	27.66	44.12
Source	54.77	66.93	29.62	50.96	40.25	61.99	29.40	55.30	37.23	51.54	38.25	57.34
Task Analogy [11]	41.14	48.21	10.24	20.32	9.35	16.75	10.10	24.00	19.77	24.70	18.12	26.79
Param Δ [3]	50.23	60.41	20.59	40.59	18.53	31.44	21.70	49.42	30.42	40.26	28.29	44.42
ABRA (ours)	57.24	70.53	29.98	55.47	42.27	66.08	35.09	59.94	38.10	53.27	40.54	61.06

Table 2: SDGOD. Comparison of mAP and AP₅₀ across challenging condition splits. ABRA achieves the highest overall average among all baselines. Best in **bold**.

Method	Day Foggy		Dusk Rainy		Night Clear		Night Rainy		Average	
	mAP	AP ₅₀								
<i>Fine-tuning</i>	36.37	57.83	26.77	50.65	36.86	69.40	16.81	29.85	29.20	51.93
Zero shot	26.36	41.10	19.55	34.93	27.50	49.63	9.19	13.60	20.65	34.82
Source	31.75	51.41	27.63	50.34	36.38	66.70	15.28	27.52	27.76	48.99
Task Analogy [11]	26.49	41.27	18.97	34.69	27.38	49.44	9.61	14.27	20.61	34.92
Param Δ [3]	17.68	26.68	5.07	8.09	4.86	8.01	7.86	12.60	8.87	13.85
ABRA (ours)	32.35	53.81	27.99	51.39	35.94	66.11	16.13	30.97	28.10	50.57

SDGOD Splits. Furthermore, we evaluate our approach on the SDGOD dataset splits, with results presented in Tab. 2. The challenging adverse conditions, particularly Night Rainy, cause severe performance drops for the *Zero shot* baseline. Consistent with our previous observations, existing task-vector methods fail to adapt effectively: Task Analogy [11] stalls at zero-shot levels, while Param Δ [3] suffers a severe performance collapse across all splits. Conversely, **ABRA** demonstrates strong robustness, surpassing the *Source* baseline overall and achieving the highest performance across the Day Foggy, Dusk Rainy, and Night Rainy conditions. While the *Source* baseline performs marginally better on the Night Clear split, **ABRA** remains highly competitive and delivers the highest overall average mAP, closely tracking the *Fine-tuning* upper bound.

5.3 Additional Analysis

Domain Design Choice. To validate the design choices behind our domain experts, we conduct an ablation study comparing models trained via the proposed Objectification strategy against two alternatives. First, we establish an initial baseline (*Zero Shot w/ Obj.*) by combining bounding boxes generated via Objectification with those produced in a zero-shot manner by θ_0 , the pretrained version of Grounding DINO. Second, we fine-tune the network using the actual semantic labels of the *Supervised* categories—rather than a unified generic label (*Supervised*). As demonstrated in Tab. 3, both retaining the original ground-

Table 3: Domain expert ablation. Evaluating objectification and class visibility strategies. ABRA yields the highest performance on unseen classes.

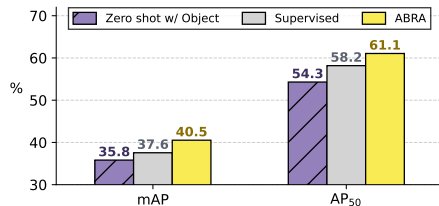


Table 4: Impact of initialization. Initializing downstream tasks (FFT or FDA [35]) with ABRA consistently outperforms standard θ_0 pretraining.

Method	Init.	mAP	AP ₅₀
FFT	θ_0	41.36	62.48
FFT	ABRA	42.80	62.77
FDA	θ_0	38.25	57.80
FDA	ABRA	40.74	61.35

truth semantics and relying on zero-shot predictions inherently restrict transferability to *unavailable* classes. Ultimately, *Objectification* achieves the highest overall performance, confirming that isolating class-agnostic visual cues is essential for effective zero-shot cross-domain adaptation.

ABRA for Downstream Tasks. Moving forward, we demonstrate that ABRA serves as a superior foundation for downstream optimization. To validate this, we use our transportable class-specific residuals to initialize two distinct strategies: supervised Full Fine-Tuning (FFT) and Unsupervised Domain Adaptation, specifically adopting the widely recognized Fourier Domain Adaptation (FDA) [35] method for the latter. As detailed in Tab. 4, weights initialized via ABRA consistently yield a higher performances than the standard pretrained backbone θ_0 across both methods, establishing a fundamentally more robust starting point for target-specific learning.

Effect of specialization.

To demonstrate the flexibility and efficacy of our class-specific approach, we evaluate a baseline configuration where a single unified expert is trained to comprehend and transport all target classes simultaneously (denoted as “Merge”). As shown in Fig. 4, our framework remains functional even without class-level specialization, successfully adapting to the target domain to some degree. However, dedicating a distinct, lightweight expert per class consistently yields higher AP₅₀ scores across all categories. The advantages of this isolation are particularly evident in complex categories; for instance, while the performance gap is moderate for classes like Rider, the specialized approach provides substantial improvements for Train and Bus. This confirms that, although our framework is capable of operating with a merged expert, allocating compact residuals to individual classes remains the optimal strategy.

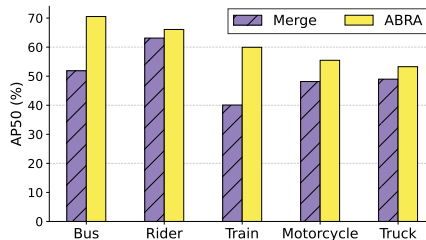


Fig. 4: Effect of specialization on Cityscapes. Dedicating one expert per class (ABRA) yields higher AP₅₀ than using a single unified expert (Merge).

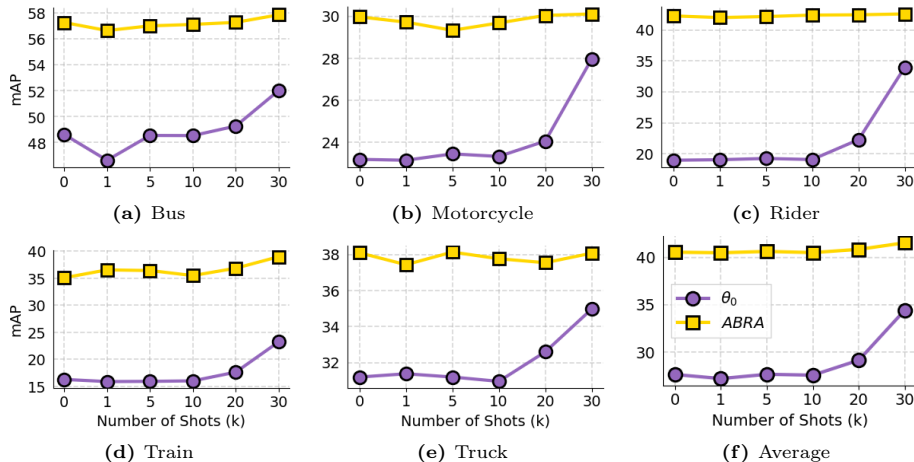


Fig. 5: Few-shot transfer evaluation. Cityscapes comparison (mAP) between the standard pretrained backbone (θ_0) and ABRA across varying numbers of shots.

Few-Shot Transfer Evaluation. Ultimately, to further investigate the transfer learning capabilities of our method, we evaluate performance in the few-shot setting, starting from both the standard pretrained checkpoint (θ_0) and our proposed approach. We focus on adapting to the target domain classes using 1, 5, 10, 20, and 30 shots. The results are presented in Fig. 5, showing the class-specific mAP and the overall average performance. As illustrated, ABRA consistently outperforms the standard θ_0 initialization across all few-shot scenarios and all evaluated categories. As the number of shots increases, both methods show gradual improvement in detection performance. However, ABRA maintains its substantial performance lead over θ_0 at every single increment tested. The average mAP results in Fig. 5f clearly demonstrate that ABRA delivers a superior performance trajectory throughout the entire few-shot learning process.

6 Conclusions

We introduced **Aligned Basis Relocation for Adaptation (ABRA)**, a novel framework for knowledge transfer across domains, addressing the challenging scenario in which no target-domain data is available. Our approach builds on the concept of *Objectification* to derive domain experts, and leverages *Specialization* through SVFT to encode class knowledge efficiently within the source domain. We then proposed a closed-form transport mechanism based on SVD decomposition and rotation alignment, enabling the relocation of class-specific information to the target domain without any additional training. Comprehensive experiments on multiple shift scenarios demonstrate that ABRA delivers strong and consistent transfer performance across multiple adverse conditions. Looking forward, we aim to develop more stable and expressive domain representations to further enhance robustness in more extreme domain-shift scenarios.

References

1. Ainsworth, S.K., Hayase, J., Srinivasa, S.: Git re-basin: Merging models modulo permutation symmetries. *International Conference on Learning Representations Workshop* (2023)
2. Bansal, Y., Nakkiran, P., Barak, B.: Revisiting model stitching to compare neural representations. *Neural Information Processing Systems* (2021)
3. Cao, S., Wu, M., Prasad, K., Tian, Y., Liu, Z.: Param delta for direct weight mixing: Post-train large language model at zero cost. *International Conference on Learning Representations Workshop* (2025)
4. Cappellino, C., Mancusi, G., Mosconi, M., Porrello, A., Calderara, S., Cucchiara, R.: Dithub: A modular framework for incremental open-vocabulary object detection. *Neural Information Processing Systems* (2025)
5. Cordts, M., Omran, M., Ramos, S., Rehfeld, T., Enzweiler, M., Benenson, R., Franke, U., Roth, S., Schiele, B.: The cityscapes dataset for semantic urban scene understanding. In: *Proceedings of the IEEE conference on Computer Vision and Pattern Recognition* (2016)
6. Deng, J., Zhang, H., Ding, K., Hu, J., Zhang, X., Wang, Y.: Zero-shot generalizable incremental learning for vision-language object detection. In: *Neural Information Processing Systems* (2024)
7. Deng, J., Li, W., Duan, L.: Balanced teacher for source-free object detection. *IEEE Transactions on Circuits and Systems for Video Technology* (2024)
8. Gu, X., Lin, T.Y., Kuo, W., Cui, Y.: Open-vocabulary object detection via vision and language knowledge distillation. In: *International Conference on Learning Representations Workshop* (2022)
9. Hernandez, A., Dangovski, R., Lu, P.Y., Soljagic, M.: Model stitching: Looking for functional similarity between representations. In: *Neural Information Processing Systems Workshops* (2022)
10. Hu, E.J., Shen, Y., Wallis, P., Allen-Zhu, Z., Li, Y., Wang, S., Wang, L., Chen, W., et al.: Lora: Low-rank adaptation of large language models. *International Conference on Learning Representations Workshop* (2022)
11. Ilharco, G., Ribeiro, M.T., Wortsman, M., Schmidt, L., Hajishirzi, H., Farhadi, A.: Editing models with task arithmetic. In: *International Conference on Learning Representations Workshop* (2023)
12. Kennerley, M., Wang, J.G., Veeravalli, B., Tan, R.T.: Cat: Exploiting inter-class dynamics for domain adaptive object detection. In: *Proceedings of the IEEE conference on Computer Vision and Pattern Recognition* (2024)
13. Kopiczko, D.J., Blankevoort, T., Asano, Y.M.: Vera: Vector-based random matrix adaptation. In: *International Conference on Learning Representations Workshop* (2024)
14. Li, L.H., Zhang, P., Zhang, H., Yang, J., Li, C., Zhong, Y., Wang, L., Yuan, L., Zhang, L., Hwang, J.N., et al.: Grounded language-image pre-training. In: *Proceedings of the IEEE conference on Computer Vision and Pattern Recognition* (2022)
15. Li, Y., Han, S., Ji, S.: Vb-lora: Extreme parameter efficient fine-tuning with vector banks. *Neural Information Processing Systems* (2024)
16. Lingam, V.C., Neerkaje, A., Vavre, A., Shetty, A., Gudur, G.K., Ghosh, J., Choi, E., Dimakis, A., Bojchevski, A., Sanghavi, S.: Svft: Parameter-efficient fine-tuning with singular vectors. *Neural Information Processing Systems* (2024)

17. Liu, S.Y., Wang, C.Y., Yin, H., Molchanov, P., Wang, Y.C.F., Cheng, K.T., Chen, M.H.: Dora: Weight-decomposed low-rank adaptation. In: International Conference on Machine Learning (2024)
18. Liu, S., Zeng, Z., Ren, T., Li, F., Zhang, H., Yang, J., Jiang, Q., Li, C., Yang, J., Su, H., et al.: Grounding DINO: Marrying dino with grounded pre-training for open-set object detection. In: Proceedings of the European Conference on Computer Vision (2024)
19. Mattolin, G., Zanella, L., Ricci, E., Wang, Y.: Confmix: Unsupervised domain adaptation for object detection via confidence-based mixing. In: Winter Conference on Applications of Computer Vision (2023)
20. Meng, F., Wang, Z., Zhang, M.: Pissa: Principal singular values and singular vectors adaptation of large language models. Neural Information Processing Systems (2024)
21. Minderer, M., Gritsenko, A., Stone, A., Neumann, M., Weissenborn, D., Dosovitskiy, A., Mahendran, A., Arnab, A., Dehghani, M., Shen, Z., et al.: Simple open-vocabulary object detection. In: Proceedings of the European Conference on Computer Vision (2022)
22. Ortiz-Jimenez, G., Favero, A., Frossard, P.: Task arithmetic in the tangent space: Improved editing of pre-trained models. Neural Information Processing Systems (2023)
23. Pan, Z., Cai, J., Zhuang, B.: Stitchable neural networks. In: Proceedings of the IEEE conference on Computer Vision and Pattern Recognition (2023)
24. Pfeiffer, J., Ruder, S., Vulić, I., Ponti, E.: Modular deep learning. Transactions on Machine Learning Research (2023)
25. Radford, A., Kim, J.W., Hallacy, C., Ramesh, A., Goh, G., Agarwal, S., Sastry, G., Askell, A., Mishkin, P., Clark, J., et al.: Learning transferable visual models from natural language supervision. In: International Conference on Machine Learning (2021)
26. Rinaldi, F., Capitani, G., Bonicelli, L., Crisostomi, D., Bolelli, F., Ficarra, E., Rodola, E., Calderara, S., Porrello, A.: Update your transformer to the latest release: Re-basin of task vectors. International Conference on Machine Learning (2025)
27. Sakaridis, C., Dai, D., Van Gool, L.: Semantic foggy scene understanding with synthetic data. International Journal of Computer Vision (2018)
28. Sangineto, E., Nabi, M., Culibrk, D., Sebe, N.: Self paced deep learning for weakly supervised object detection. IEEE Transactions on Pattern Analysis and Machine Intelligence (2019)
29. Stoica, G., Bolya, D., Bjorner, J.B., Ramesh, P., Hearn, T., Hoffman, J.: Zipit! merging models from different tasks without training. In: International Conference on Learning Representations Workshop (2024)
30. Tang, S., Yang, J., Ye, M., Wang, B., Gan, Y., Zhu, X.: Source-free domain adaptive object detection with semantics compensation. arXiv preprint arXiv:2410.05557 (2025)
31. Tarvainen, A., Valpola, H.: Mean teachers are better role models: Weight-averaged consistency targets improve semi-supervised deep learning results. In: Neural Information Processing Systems (2017)
32. Van de Ven, G.M., Tuytelaars, T., Tolias, A.S.: Three types of incremental learning. Nature Machine Intelligence (2022)
33. Wu, A., Deng, C.: Single-domain generalized object detection in urban scene via cyclic-disentangled self-distillation. In: Proceedings of the IEEE conference on Computer Vision and Pattern Recognition (2022)

34. Wu, A., Deng, C.: Single-domain generalized object detection in urban scene via cyclic-disentangled self-distillation. In: Proceedings of the IEEE conference on Computer Vision and Pattern Recognition (2022)
35. Yang, Y., Soatto, S.: Fda: Fourier domain adaptation for semantic segmentation. In: Proceedings of the IEEE conference on Computer Vision and Pattern Recognition (2020)
36. Yuan, Y., Tang, L., Chen, Y., Chen, C., Huang, Y., Ding, X.: Asgs: Single-domain generalizable open-set object detection via adaptive subgraph searching. In: IEEE International Conference on Computer Vision (2025)
37. Zang, Y., Li, W., Zhou, K., Huang, C., Loy, C.C.: Open-vocabulary detr with conditional matching. In: Proceedings of the European Conference on Computer Vision (2022)
38. Zhang, H., Cisse, M., Dauphin, Y.N., Lopez-Paz, D.: mixup: Beyond empirical risk minimization. In: International Conference on Learning Representations Workshop (2018)
39. Zhang, R., Chen, T., Shen, Y., Carin, L., Wang, W., Chen, W.: Adaptive low-rank adaptation of pretrained models. In: International Conference on Learning Representations Workshop (2023)
40. Zhong, Y., Yang, J., Zhang, P., Li, C., Codella, N., Li, L.H., Zhou, L., Dai, X., Yuan, L., Li, Y., et al.: Regionclip: Region-based language-image pretraining. In: Proceedings of the IEEE conference on Computer Vision and Pattern Recognition (2022)
41. Zhou, X., Girdhar, R., Joulin, A., Krähenbühl, P., Misra, I.: Detecting twenty-thousand classes using image-level supervision. In: Proceedings of the European Conference on Computer Vision (2022)

ABRA: Teleporting Fine-Tuned Knowledge Across Domains for Open-Vocabulary Object Detection

Supplementary Material

A Orthogonal Alignment of Singular Subspaces

Given source and target singular subspaces

$$U_S, U_T \in \mathbb{R}^{n \times k}, \quad U_S^\top U_S = U_T^\top U_T = I_k,$$

our goal is to align them through an orthogonal transformation $L \in \mathbb{R}^{k \times k}$ acting in the reduced k -dimensional space. We seek the orthogonal matrix that best maps the target basis onto the source basis:

$$\min_{L^\top L = I_k} \|U_S - U_T L\|_F^2. \quad (13)$$

Expanding the Frobenius norm and using $U_S^\top U_S = U_T^\top U_T = I_k$ yields a standard simplification:

$$\|U_S - U_T L\|_F^2 = 2k - 2 \operatorname{tr}(U_S^\top U_T L). \quad (14)$$

Since $2k$ is constant, solving (13) is equivalent to

$$\max_{L^\top L = I_k} \operatorname{tr}(L^\top M), \quad M := U_T^\top U_S. \quad (15)$$

Let $M = U \Sigma V^\top$ be the SVD. The orthogonal Procrustes solution directly gives

$$L^* = UV^\top. \quad (16)$$

Our use of the alignment. We use L^* to rotate the target singular basis into the source space:

$$\tilde{U}_T = U_T L^*,$$

ensuring that the two subspaces are optimally aligned in the least-squares sense while preserving geometric structure (orthogonality, scale). This aligned basis is what we feed into our adaptation module.

Special case. If U_T and U_S span the same subspace, then M is already orthogonal and the solution reduces to:

$$L^* = U_T^\top U_S.$$

This is simply the Procrustes solution applied to an already perfectly matched pair of subspaces.

B Implementation Details

ABRA and the compared baselines all adapt Grounding DINO as the pretrained OVD backbone. Domain checkpoints are derived by fine-tuning only the encoder attention layers for 10 epochs, utilizing a standard learning rate of $1e-4$, a batch size of $\mathcal{B} = 2$, and a weight decay of $1e-4$. Starting from the source-domain expert, we perform class specialization via SVFT by training these same attention layers for an additional 12 epochs with an increased learning rate of $1e-2$ and $\mathcal{B} = 4$. For these class experts, we do not apply weight decay and utilize the banded pattern of SVFT with an off-diagonal value (`off_diag`) of 2. During both the domain and class expert training phases, we employ a multi-step learning rate scheduler that drops the learning rate by a factor of 10 at epochs 7 and 9. Additionally, the specific layers `ref_point_head` and `sampling_offset` are always assigned an initial learning rate reduced by a factor of 10 with respect to the standard learning rate across both stages.

C Qualitative Results

In this section, we provide additional qualitative results to further demonstrate the effectiveness of our proposed approach, ABRA. Table Tab. 5 illustrates a visual comparison between the source-only baseline, our method, and the ground truth (GT) on challenging examples from the target domain, which features severe fog and reduced visibility. As observed in the leftmost column, the baseline model struggles significantly under these adverse weather conditions. It fails to detect or correctly classify difficult and heavily obscured objects, entirely missing the bus (top row), rider (middle row), and train (bottom row). Conversely, our proposed method (middle column) successfully localizes and classifies these challenging instances. Despite the dense fog and domain shift, ABRA generates bounding box predictions that closely match the ground truth annotations (rightmost column).



Table 5: Top to bottom: bus, rider, train. Left to right: source (baseline), ABRA, GT